

Level density and γ -ray strength in $^{27,28}\text{Si}$

M. Guttormsen[†], E. Melby, J. Rekstad, and S. Siem

Department of Physics, University of Oslo, N-0316 Oslo, Norway

A. Schiller

Lawrence Livermore National Laboratory, L-414, 7000 East Avenue, Livermore
CA-94551, USA

T. Lönnroth

Department of Physics, Åbo Akademi, FIN-20500 Turku, Finland

A. Voinov

Frank Laboratory of Neutron Physics, Joint Institute of Nuclear Research, 141980
Dubna, Moscow reg., Russia

Abstract. A method to extract simultaneously level densities and γ -ray transmission coefficients has for the first time been tested on light nuclei utilizing the $^{28}\text{Si}(^3\text{He},\alpha\gamma)^{27}\text{Si}$ and $^{28}\text{Si}(^3\text{He},^3\text{He}'\gamma)^{28}\text{Si}$ reactions. The extracted level densities for ^{27}Si and ^{28}Si are consistent with the level densities obtained by counting known levels in the respective nuclei. The extracted γ -ray strength in ^{28}Si agrees well with the known γ -decay properties of this nucleus. Typical nuclear temperatures are found to be $T \sim 2.4$ MeV at around 7 MeV excitation energy. The entropy gap between nuclei with mass number A and $A\pm 1$ is measured to be $\delta S \sim 1.0 k_B$, which indicates an energy spacing between single-particle orbitals comparable with typical nuclear temperatures.

Submitted to: *J. Phys. G: Nucl. Phys.*

PACS numbers: 21.10.Ma, 21.10.Pc, 24.10.Pa, 27.30.+t

[†] To whom correspondence should be addressed (magne.guttormsen@fys.uio.no)

1. Introduction

The Oslo Cyclotron group has developed a method to extract first-generation (primary) γ -ray spectra at various initial excitation energies [1]. From the set of primary spectra, nuclear level densities and γ -ray strength functions can be extracted [2, 3]. These two functions reveal essential nuclear structure information such as shell gaps, pair correlations, and thermal and electromagnetic properties. In the last couple of years, the Oslo group has demonstrated several fruitful applications of the method [4, 5, 6, 7, 8, 9, 10, 11, 12].

So far, the method has been tested on rare earth nuclei, having a rather uniform and high single-particle level density. These properties are expected to be important for the foundation of the method. The two crucial steps in the extraction procedure are: (i) the subtraction technique for obtaining the primary γ -ray spectra, and (ii) the Brink-Axel hypothesis telling that nuclear resonances with approximately equal properties can be built on all states. Thus, the most important requirements are that the spin and parity distributions should be similar for all excitation energy bins and that the nucleus should thermalize at each step within a given γ cascade.

Although not finally validated, the method has been tested and found successful for deformed rare-earth nuclei [4, 5, 6, 7, 8, 9, 10, 11] and even for the weakly deformed $^{148,149}\text{Sm}$ nuclei [12]. However, in cases where the statistical properties are less favourable, as for lighter nuclei and/or for nuclei in the vicinity of closed shells, the foundation of the method is more doubtful. Since both ^{27}Si and ^{28}Si of the present study are open-shell systems in the middle of the sd shell, only the statistical question remains here.

From a statistical point of view it is important that for light nuclei having low level density one can expect a strong influence of Porter-Thomas fluctuations on γ -transition intensities of primary γ spectra and hence, on extracted level densities and γ -ray strength functions. This means that the main assumptions of the Oslo method can fail, namely that the applicability of the Axel-Brink hypothesis can lose its meaning because of large γ -intensity fluctuations and insufficient averaging over nuclear levels due to a low level density. From this point of view it is interesting to establish the limit of the applicability of the Oslo method by investigating light nuclei.

In this work, we have tested the extraction procedure on the light ^{27}Si and ^{28}Si systems, applying the $(^3\text{He},\alpha)$ pick-up reaction and the $(^3\text{He},^3\text{He}')$ inelastic scattering reaction, respectively. Since both the level density and the γ -decay rates are known in these nuclei, a quantitative judgment of the applicability of the procedure is feasible. Section 2 describes the experimental methods and techniques, and in sections 3 and 4 the level density and γ -ray strength are discussed. Finally, concluding remarks are given in section 5.

2. Experimental method and techniques

The experiment was carried out at the Oslo Cyclotron Laboratory with a 45 MeV ^3He beam. The self-supporting ^{28}Si target was isotopically enriched to 100% and had a thickness of 3 mg/cm². The reactions employed in the extraction procedure were $^{28}\text{Si}(^3\text{He},\alpha\gamma)^{27}\text{Si}$ and $^{28}\text{Si}(^3\text{He},^3\text{He}'\gamma)^{28}\text{Si}$.

The charged particles and γ rays were recorded with the detector array CACTUS, which contains eight particle telescopes, 27 NaI γ -ray detectors and two additional Ge detectors monitoring the spin distribution and the selectivity of the reactions. Each telescope is placed at an angle of 45° relative to the beam axis, and comprises one Si front and one Si(Li) back detector with thicknesses of 140 and 3000 μm , respectively. The NaI γ -detector array surrounding the target and particle detectors has a resolution of $\sim 6\%$ at $E_\gamma = 1$ MeV and a total efficiency of $\sim 15\%$.

In figures 1 and 2, the single and coincidence ejectile spectra are shown for the reactions $^{28}\text{Si}(^3\text{He},\alpha)^{27}\text{Si}$ and $^{28}\text{Si}(^3\text{He},^3\text{He}')^{28}\text{Si}$, respectively. The ground state in ^{27}Si is located at higher ejectile energy due to a positive Q value of 3.40 MeV in the $(^3\text{He},\alpha)$ reaction. In ^{27}Si and ^{28}Si , pronounced peak structures are seen up to 5 and 10 MeV excitation energy, respectively. The coincident spectra show a drop in yield at the proton binding energies B_p , since the residual nucleus with one proton less (aluminium) is then populated at low excitation energy with a corresponding low γ -ray multiplicity. Our extraction method is therefore only applicable up to the excitation energy of $E \sim B_p$. The spin window of the present pick-up and elastic scattering reactions is concentrated at $I \sim 2 - 4\hbar$.

In order to determine the true γ -energy distribution, the γ spectra are corrected for the response of the NaI detectors with the unfolding procedure of [13]. In addition, random coincidences are subtracted from the γ spectra. The resulting unfolded NaI γ spectra are shown in figure 3. The spectra reveal strong γ lines, which are identified as transitions between low-lying states.

The set of unfolded γ spectra are organized in a (E, E_γ) matrix, where the initial excitation energies E of ^{27}Si and ^{28}Si are determined by means of reaction kinematics, utilizing the energy of the ejectile. This matrix comprises the γ -energy distribution of the total γ cascade. The primary- γ matrix can now be found according to the subtraction technique of [1].

As indicated in the introduction, the primary γ -ray procedure is based on the assumption that the decay properties of the particular reaction-selected distribution of states within each energy bin are independent on whether the respective ensembles of states are directly populated through the nuclear reaction or by γ decay from higher-lying states. In the present case, the γ -ray multiplicity is low and reaches $M_\gamma \sim 2$ around 10 MeV excitation energy. Thus, generally less than half of the counts in the total γ spectra have to be subtracted in the procedure, giving quite reliable primary γ -ray spectra. This is demonstrated in figure 4, where we compare our results to known γ -decay branches from various excitation-energy regions [14]. Here, in the reconstruction

of primary γ spectra from known γ transitions, we have assumed equal population of the initial levels within each energy bin. Taking into account that probably not all levels and branchings are known, the agreement is very satisfactory. It should be noted that possible Porter-Thomas fluctuations will reveal themselves in exactly the same way in the literature data and the extracted primary γ spectra. Thus, agreement between the two spectra of figure 4 should not be surprising from a statistical point of view.

The idea is now to find two functions, the level density $\rho(E)$ and the γ -energy-dependent function $\mathcal{T}(E_\gamma)$, that, multiplied with each other, reproduce the set of primary γ -ray spectra. The $\mathcal{T}(E_\gamma)$ function is identified as the so-called γ -ray transmission coefficient. According to the Brink-Axel hypothesis [15, 16], the primary γ -ray spectra can be factorized by

$$P(E, E_\gamma) \propto \rho(E - E_\gamma)\mathcal{T}(E_\gamma), \quad (1)$$

where $P(E, E_\gamma)$ is fitted to the primary γ -ray matrix by a least χ^2 fit [3]. In the factorization procedure, we use primary spectra from the initial excitation-energy regions of $E = 3.6\text{--}7.6$ MeV and $E = 4.2\text{--}12.1$ MeV for ^{27}Si and ^{28}Si , respectively. The corresponding γ -energy regions were chosen to be $E_\gamma = 1.1\text{--}7.6$ MeV and $E_\gamma = 2.2\text{--}12.1$ MeV.

In figure 5, the best fits (solid lines) to the experimental P are shown for the ^{27}Si and ^{28}Si nuclei. The experimental spectra exhibit strong peak structures that are in good correlation in spite of the fact that they have been obtained at different excitation energies. The correlation indicates that the peak structures are mainly due to the γ -ray transmission coefficient $\mathcal{T}(E_\gamma)$ which is assumed to be independent of the excitation energies of initial and final states. This is also supported by the fact that the highly structured experimental spectra are seen to be fairly well described by the factorization in equation (1). The expected Porter-Thomas fluctuations can be estimated from the deviations of the experimental points from the solid line in figure 5, which demonstrate that the fluctuations are of minor importance for the extracted level densities and γ -ray transmission coefficients.

In our extraction procedure, we assume that the γ -ray transmission coefficient $\mathcal{T}(E_\gamma)$ is independent of the excitation energy (or temperature). Although no strict violation of this assumption has been determined experimentally, theoretical predictions show that $\mathcal{T}(E_\gamma)$ may depend on the thermal properties of the final state. In order to estimate the influence of such effects, we have applied the temperature dependent model of Kadenskii, Markushev and Furman [17] for electric dipole transitions. The model describes a γ -ray strength function based on the low energy tail of the giant electric dipole resonance (GEDR), where we use GEDR parameters from [18]. To evaluate the temperature at a certain excitation energy, we use $T = \sqrt{U/a}$, where U and a are the intrinsic excitation energy and the level density parameter, respectively. These parameters are determined according to von Egidy *et al.* [19]. In our experiment, we measure γ spectra from a certain initial excitation energy E , and the temperature T is determined by the excitation energy of the final state $E - E_\gamma$. Since we use spectra from

several E for a given E_γ , also the final excitation energy will change accordingly, giving different temperatures for different γ energies. For the tests, we used the KMF model including this variation in temperature with γ energies, and compared with a calculation where the temperature is kept constant. Here, we find for ^{28}Si that the $\mathcal{T}_{\text{KMF}}(E_\gamma)$ values deviate within 20 % for $E_\gamma > 3$ MeV. However, for lower E_γ the $\mathcal{T}_{\text{KMF}}(E_\gamma)$ value with variable temperature increases and gains a factor of two at $E_\gamma = 2$ MeV compared to the value of $\mathcal{T}_{\text{KMF}}(E_\gamma)$ taken at a constant temperature. The varying temperature is associated with a standard deviation of ~ 0.4 MeV, which will reduced this difference somewhat. Since the predicted temperature dependence is highly uncertain, if existing at all in real silicon nuclei, we omit to include this uncertainty in the experimental error bars.

The multiplicative functions $\rho(E)$ and $\mathcal{T}(E_\gamma)$ of equation (1) are not uniquely determined. Actually, one may construct an infinite number of other functions [3], which give identical fits to the data of figure 5 by

$$\tilde{\rho}(E - E_\gamma) = A \exp[\alpha(E - E_\gamma)] \rho(E - E_\gamma), \quad (2)$$

$$\tilde{\mathcal{T}}(E_\gamma) = B \exp(\alpha E_\gamma) \mathcal{T}(E_\gamma). \quad (3)$$

Consequently, neither the slope nor the absolute value of the two functions can be obtained through the fitting procedure. Thus, the free parameters A , B and α have to be determined from other information to give the best physical solution.

3. Level density

The ^{27}Si and ^{28}Si nuclei have been thoroughly studied during the last decades, and the level schemes are probably fairly complete up to several MeV excitation energy. By smoothing the known level density taken from the database of [14] with the experimental energy resolution, we can adjust the parameters A and α of our experimental ρ to fit the level density to the number of known levels. The adjustments were performed at $E = 0.9$ and 5.0 MeV in ^{27}Si and at $E = 1.7$ and 7.0 MeV in ^{28}Si . These anchor points are well determined and separated in excitation energy, however, also other data points could as well be used.

Figure 6 compares cumulated number of levels based on our data (data points) and known levels (histogram) taken from [14]. The overall agreement is gratifying*. Local differences can be caused by violation of the Axel-Brink hypotheses for light nuclei, where low level density and large fluctuations of γ intensity is observed. For example, in ^{28}Si , the level density around the ground state is strongly underestimated in the experiment, because very few transitions decay directly to the $I^\pi = 0^+$ ground state. This property is less pronounced in ^{27}Si , having a ground state assignment of $I^\pi = 5/2^+$. Since these nuclei have been well studied, we are not able to extract much more information on the level density than what is already known. However, our data

* Apparently, our data seem to be wrong adjusted to the anchor point at $E = 1.7$ MeV in ^{28}Si , but the plot shows cumulated numbers of levels and not level densities.

give a small indication that not all levels in ^{28}Si have yet been observed above 9 MeV excitation energy.

Very few explicit calculations of level densities exist. This would be needed, since a simple Fermi-gas approximation based on the level-density parameter a and the pairing-gap parameter Δ neglects residual interactions. In the calculations of Ormand [20], the level densities of ^{24}Mg and ^{32}S were studied in a Monte-Carlo Shell-Model approach within the sd shell. It is interesting that the level density in ^{24}Mg behaves very much like the nuclei studied here. The fact that there are only one hundred levels per MeV at excitation energies of 8–12 MeV has implications. It indicates that if specific states are selected by some reaction, e.g., α -cluster states with large parentage of $\pi^2\nu^2$ configurations, the number of states of this kind necessarily must be significantly lower. However, at this stage, it is not possible to give quantitative statements of the number of, e.g., α -cluster states in this region.

In general, the most successful way to create additional states in atomic nuclei is to break up $J = 0$ nucleon Cooper pairs. Each broken pair increases the level density by a factor of 10-20, which is much higher than obtained from other modes of excitation as, e.g., rotation or vibration. Recently [9, 21, 22], a thermodynamic model was developed which could describe level densities for mid-shell nuclei in the mass regions $A = 58, 106, 162,$ and 234 . The model is based on the canonical ensemble theory, where equilibrium is obtained at a certain given temperature T .

The basic idea of the model [9, 21, 22] is the assumption of a reservoir of proton and neutron pairs. The pairs may be broken such that unpaired nucleons are thermally scattered into an infinite, equidistant, doubly-degenerated single-particle level scheme. In addition, rotational and vibrational modes may be thermally excited. The total partition function is written as a product of proton (Z_π), neutron (Z_ν), rotation (Z_{rot}), and vibration (Z_{vib}) partition functions. Then, from the Helmholtz free energy

$$F(T) = -T \ln (Z_\pi Z_\nu Z_{\text{rot}} Z_{\text{vib}}), \quad (4)$$

thermodynamical quantities as entropy, average excitation energy, and heat capacity can be calculated as

$$S(T) = - \left(\frac{\partial F}{\partial T} \right)_V \quad (5)$$

$$\langle E(T) \rangle = F + ST \quad (6)$$

$$C_V(T) = \left(\frac{\partial \langle E \rangle}{\partial T} \right)_V, \quad (7)$$

where the Boltzmann constant is set to unity ($k_B = 1$) and the temperature T is measured in MeV. The level density is calculated applying the saddle-point approximation [23]

$$\rho(\langle E \rangle) = \frac{\exp(S)}{T \sqrt{2\pi C_V}}. \quad (8)$$

The energy spacing between the single-particle orbitals ε is the most critical parameter of the model. In order to determine ε , we investigate the well-studied ^{26}Al

and ^{27}Al isotopes, where the level density is presumably known up to high excitation energy from the counting of experimentally observed levels [14]. Figure 7 shows these experimental data together with a level-density point evaluated for ^{28}Al [9] from the average neutron-resonance spacing [24] at the neutron binding energy B_n . The slopes of the level densities are well reproduced with $\varepsilon = 2.0$ MeV, which is consistent with the energy gaps in the Nilsson single-particle level scheme. The difference in level density between ^{26}Al and ^{27}Al depends strongly on the pairing-gap energy and is well described by a gap parameter of $\Delta = 12A^{-1/2}$ MeV = 2.3 MeV, using $A = 28\ddagger$.

The pairing-attenuation factor, defined as the ratio between the amount of energy needed to break one nucleon pair compared to the previous broken pair, is set to $r = 0.56$ (for details see [22]). For simplicity, we have used the same values of ε , Δ , and r for protons and neutrons. Furthermore, all calculations include a reservoir of seven proton and seven neutron pairs. The collective parameters are taken from experimental data on ^{28}Si . The rotational parameter $A_{\text{rot}} = E/2(2+1) = 0.3$ MeV is calculated from the first excited state ($I^\pi = 2^+$), and the vibrational energy $\hbar\omega_{\text{vib}} = 5.0$ MeV is set equal to the excitation energy of the first non-rotational state ($I^\pi = 0^+$).

The very same parameter set is used in the calculation for ^{27}Si and ^{28}Si in figure 8. The calculation describes well the experimental data of ^{27}Si for excitation energies above $E \sim 4$ MeV. For ^{28}Si , the more statistical and smooth part of the level density takes place first above $E \sim 9$ MeV, making it difficult to judge the agreement between model and experiment in this case.

By comparing the level densities between even-even (^{28}Si), odd- A (^{27}Al or ^{27}Si), and odd-odd (^{26}Al) systems§, we may extract interesting information. In figure 9, the free energy F , entropy S , average excitation energy $\langle E \rangle$, and heat capacity C_V are shown as functions of temperature for the three systems. A fruitful quantity is the entropy difference δS between systems with A and $A \pm 1$. At low temperatures, this quantity is approximately extensive (additive) and represents the single-particle entropy associated with the valence particle (or hole) [9]. In the upper right panel, we find that the nucleon carries a single-particle entropy of $\delta S \sim 1.0$ at $T \sim 1.5$ MeV.

The single-particle entropy can also be deduced from the experimental data of aluminium (and possibly also from silicon). The high-energy data points of figure 7 reveal that the level density of ^{26}Al is ~ 2.7 times higher than for ^{27}Al . Remembering that the level density and entropy are connected by

$$S = \ln \rho + \text{constant}, \quad (9)$$

‡ It is difficult to determine an appropriate pairing gap parameter in this mass region. If one calculates pairing gap parameters Δ_p and Δ_n from nuclear mass differences [25], the various systems give strongly scattered values. This mainly reflects the variation in the distance between the Fermi level and neighbouring single particle states [26], which could in principle be as high as $\varepsilon \sim 2.0$ MeV. Since this distance is schematically included in our model, we adopt here the "pure" pairing contribution of approximately $\Delta = 12A^{-1/2}$ MeV, which represents an average value in this mass region.

§ The proton and neutron parameters are identical and give no difference between odd-even and even-odd systems. We therefore denote either of these two systems as the odd- A system.

we deduce also here $\delta S \sim 1.0$.

The statistical definition of temperature in the microcanonical ensemble is given by

$$T = \left(\frac{\partial S}{\partial E} \right)_V^{-1}, \quad (10)$$

giving typically $T \sim 2.4$ MeV for the data points of ^{27}Al in the excitation-energy region of 7–11 MeV, see figure 7. Since the excitation-energy shift between the level densities of figure 7 amounts approximately to the pairing-gap parameter Δ , we may express the slope of $\ln(\rho)$ as $\delta S/\Delta$ or, according to equations (9) and (10), as T^{-1} , giving

$$\delta S = \Delta/T, \quad (11)$$

which again confirms $\delta S = 2.3/2.4 \sim 1.0$.

The extracted single-particle entropy is lower than observed in heavier mid-shell nuclei where typically $\delta S \sim 1.7$ [9]. The recent findings are supported by the systematics of figure 10, where the experimentally deduced level densities at $E = 7$ MeV are displayed for various nuclear systems. These data points are evaluated as a linear interpolation of $\ln \rho(E)$ between two anchor points: (i) the level density based on known levels at low excitation energy and (ii) the level density estimated from neutron resonance energy spacings at the neutron binding energy [9]. Figure 10 shows larger error bars and more scattered data for mass numbers below $A \sim 40$, which mainly reflects that the first anchor point is strongly influenced by local shell effects. However, in spite of local shell effects below $A \sim 40$, it is clear that the level densities drop one order of magnitude, and the level density gaps between various systems are severely reduced. From our model calculations, this change is due to a decrease in the ratio between the temperature T and the single-particle energy spacing ε . In the mass region studied here, the temperature and spacing are approximately equal, i.e., $T \sim \varepsilon$, and the valence nucleon is thermally smeared over the ground state and the first excited single-particle level, giving $\delta S = \ln 2 = 0.7$, only. In the rare earth region, we have typically $T \sim 3\varepsilon$ and the valence nucleon is thermally spread over several single-particle levels, giving higher entropy.

The heat-capacity curves of figure 9 show S-shaped forms, in particular for the even-even system. The local maximum of this shape appears at $T_m \sim 2.4$ MeV, corresponding to an excitation energy of $\langle E \rangle = 10$ MeV. At this point, the excitation energy increases strongly with temperature, indicating a substantial breaking of nuclear Cooper pairs. It is tempting to connect this overshoot in heat capacity with a pairing-phase transition. In order to test this, we have studied the distribution of zeros of the partition function in the complex temperature plane, as prescribed in [22, 27]. In our calculations, we find that the zeros move away from the real, inverse-temperature axis with increasing inverse temperature. This property is inconsistent with a pairing-phase transition in the thermodynamical limit of $A \rightarrow \infty$, in accordance with the generalized Ehrenfest definition of a phase transition [28]. A similar conclusion has also been drawn for the Fe mass region [22].

4. Gamma-ray strength

The γ -ray energy-dependent function $\mathcal{T}(E_\gamma)$ contains information on the average γ -decay probability. In figure 11, the non-normalized $\mathcal{T}(E_\gamma)$ of equation (3) is shown with the α parameter determined in section 3. The two extreme data points at $E_\gamma = 3.2$ and 5.0 MeV for ^{27}Si and ^{28}Si , respectively, are probably due to a singularity in the extraction method, giving too small error bars.

It has been shown [29, 30] that the regularity of the γ -decay strength in the continuum is determined by the γ -ray strength function[¶]

$$f_{XL} = \Gamma_{XL}^i(E_\gamma)/(E_\gamma^{2L+1}D^i), \quad (12)$$

where E_γ is the transition energy, X denotes the electric or magnetic character, L is the multipolarity, $\Gamma_{XL}^i(E_\gamma)$ is the partial radiative width, and D^i is the level spacing of states with spins and parities equal to those of the initial state i . The main part of high-lying levels is known to decay by $E1$ and $M1$ γ transitions. Thus, one could in principle extract $f_{E1} + f_{M1}$ from the present experiment in the same way as has been done for several rare-earth nuclei [10, 11, 12]. However, the concept of an average radiative width is difficult to adopt for these light nuclei, since there is no experimental information on the mean values of the level spacing D^i ; there are less than one level per MeV with presumably the same spin and parity.

Even though the absolute strength of f is uncertain, its functional dependence on E_γ can be studied. The shape of the measured γ -ray transmission coefficient is given by

$$\mathcal{T}(E_\gamma) = 2\pi \sum_{\lambda=1,2,\dots} [f_{E\lambda}(E_\gamma) + f_{M\lambda}(E_\gamma)] E_\gamma^{2\lambda+1}. \quad (13)$$

If the transitions are mainly governed by single-particle dipole transitions, an E_γ^3 shape would be expected according to the Weisskopf estimate, where f_{E1} and f_{M1} take constant values. The functional form is displayed in figure 11. Both ^{27}Si and ^{28}Si show a rather flat shape of \mathcal{T} for $E_\gamma < 4$ –5 MeV. However, for $E_\gamma > 4$ –5 MeV, ^{28}Si follows roughly the E_γ^3 dependence, indicating that the transitions are rather of single-particle than collective origin as found for rare-earth nuclei [10, 11, 12]. Also, the large spread in lifetimes [14] of the high-lying levels supports this interpretation.

In ^{28}Si , levels and their lifetimes and γ -decay branching ratios are known up to 9.6 MeV of excitation energy from discrete γ spectroscopy [14]. Thus, we may define the decay intensity in terms of the partial (Γ_{ij}) and total (Γ_i) decay widths by $I_{ij}(E_\gamma) = \Gamma_{ij}/\Gamma_i$, where the γ -transition energy is determined by the excitation energies of the initial (i) and final (j) states by $E_\gamma = E_i - E_j$. For this case, the γ -ray transmission coefficient reads

$$\mathcal{T}_{ij}(E_\gamma) = 2\pi\hbar I_{ij}(E_\gamma)/\tau_i D^i, \quad (14)$$

where τ_i is the lifetime of level i . Here, we roughly estimate D^i from the total level density using the spin distribution of [31]. The constructed γ -ray transmission coefficient

[¶] Also called the radiative strength function in literature.

is then smoothed as a function of E_γ with the experimental resolution. Despite the fact that not all levels and decay branches are known, figure 11 shows that the smoothed γ -ray transmission coefficient compares surprisingly well with the extracted data points. This indicates that the method may work even in cases where no well-behaving smooth γ -ray strength function is present.

5. Conclusions

A simultaneous extraction of level densities and γ -ray transmission coefficients in $^{27,28}\text{Si}$ has been performed. Comparison to literature data gives excellent agreement within the experimental resolution. This study demonstrates that the extraction method also works for light nuclei, despite the fact that thermalization might seem questionable. The concept of a γ -ray strength function in this mass region is not very useful. The measured γ -energy dependence of approximately E_γ^3 indicates that the γ decay is governed by single-particle dipole transitions.

A simple thermodynamical model reproduces the high excitation-energy region of the experimental data. For $^{27,28}\text{Si}$ and $^{26,27}\text{Al}$, we conclude that a nuclear temperature of $T \sim 2.4$ MeV and a pairing gap parameter of $\Delta \sim 2.3$ MeV describes the level densities at high excitation energies. Both experiment and model indicate that the valence nucleon in this mass region carries an entropy of $\delta S \sim 1.0$. This is close to the expected value of 0.7 when the thermal nucleonic excitation is smeared over the ground state and only one excited single-particle level. The pair breaking process is strongly smeared out in temperature (and excitation energy) and a phase transition in the sense of the Ehrenfest definition is doubtful.

The present work encourages also similar studies in the mass region $A = 30$ – 100 . Here, nuclear level densities are used in the determination of nuclear reaction cross sections from Hauser-Feshbach type of calculations. These cross sections, as well as the γ -ray strength functions, are important inputs in large network calculations of stellar evolution [32], as well as in the simulations of accelerator-driven transmutation of nuclear waste.

Acknowledgements

Financial support from the Norwegian Research Council (NFR) is gratefully acknowledged. Part of this work was performed under the auspices of the U.S. Department of Energy by the University of California, Lawrence Livermore National Laboratory under Contract No. W-7405-ENG-48. T.L. warmly acknowledges the financial support from the Magnus Ehrnrooth Foundation in Helsinki. A.V. would like to thank the staff of the University of Oslo for their warm hospitality while this manuscript was prepared and acknowledges support from a NATO Science Fellowship under project number 150027/432 given by the Norwegian Research Council (NFR).

References

- [1] Guttormsen M, Ramsøy T, and Rekstad J 1987 *Nucl. Instrum. Methods Phys. Res. A* **255**, 518
- [2] Henden L, Bergholt L, Guttormsen M, Rekstad J, and Tveter T S 1995 *Nucl. Phys.* **A589**, 249
- [3] Schiller A, Bergholt L, Guttormsen M, Melby E, Rekstad J, and Siem S 2000 *Nucl. Instrum. Methods Phys. Res. A* **447**, 498
- [4] Melby E, Bergholt L, Guttormsen M, Hjorth-Jensen M, Ingebretsen F, Messelt S, Rekstad J, Schiller A, Siem S, and Ødegård S W 1999 *Phys. Rev. Lett.* **83**, 3150
- [5] Schiller A, Guttormsen M, Melby E, Rekstad J, and Siem S 2000 *Phys. Rev. C* **61**, 044324
- [6] Guttormsen M, Hjorth-Jensen M, Melby E, Rekstad J, Schiller A, and Siem S 2000 *Phys. Rev. C* **61**, 067302
- [7] Guttormsen M, Bjerve A, Hjorth-Jensen M, Melby E, Rekstad J, Schiller A, Siem S, and Belić A 2000 *Phys. Rev. C* **62**, 024306
- [8] Schiller A, Bjerve A, Guttormsen M, Hjorth-Jensen M, Ingebretsen F, Melby E, Messelt S, Rekstad J, Siem S, and Ødegård S W 2001 *Phys. Rev. C* **63**, 02130
- [9] Guttormsen M, Hjorth-Jensen M, Melby E, Rekstad J, Schiller A, and Siem S 2001 *Phys. Rev. C* **63**, 044301
- [10] Melby E, Guttormsen M, Rekstad J, Schiller A, Siem S, and A. Voinov 2001 *Phys. Rev. C* **63**, 044309
- [11] Voinov A, Guttormsen M, Melby E, Rekstad J, Schiller A, and Siem S 2001 *Phys. Rev. C* **63**, 044313
- [12] Siem S, Guttormsen M, Melby E, Rekstad J, Schiller A, and Voinov A 2002 *Phys. Rev. C* **65**, 044318
- [13] Guttormsen M, Tveter T S, Bergholt L, Ingebretsen F, and Rekstad J 1996 *Nucl. Instrum. Methods Phys. Res. A* **374**, 371
- [14] Data extracted using the NNDC On-Line Data Service from the ENSDF database, file revised as of Jan. 21, 2000
- [15] Brink D M 1955 Ph.D. thesis, Oxford University
- [16] Axel P 1962 *Phys. Rev.* **126**, 671
- [17] Kadenskii S G , Markushev V P, and Furman V I 1983 *Yad. Fiz.* **37**, 277 [1983 *Sov. J. Nucl. Phys.* **37**, 165]
- [18] *Handbook for calculations of nuclear reaction data*, IAEA, Vienna, 1998 IAEA-TECDOC-1024
- [19] von Egidy T, Schmidt H H, and Behkami A N 1987 *Nucl. Phys.* **A481**, 189
- [20] Ormand W E 1997 *Phys. Rev. C* **56**, R1678
- [21] Guttormsen M, Hjorth-Jensen M, Melby E, Rekstad J, Schiller A, and Siem S 2002 *Phys. Rev. C* **64**, 034319
- [22] Schiller A, Guttormsen M, Hjorth-Jensen M, Rekstad J, and Siem S 2002 *Phys. Rev. C* **66**, 024322
- [23] Nakada H and Alhassid Y 1997 *Phys. Rev. Lett.* **79**, 2939
- [24] Iljinov A S, Mebel M V, Bianchi N, De Sanctis E, Guaraldo C, Lucherini V, Muccifora V, Polli E, Reolon A R, and Rossi P 1992 *Nucl. Phys.* **A543**, 517
- [25] Bohr A, Mottelson B 1969 *Nuclear Structure* (Benjamin, New York) Vol.I, p 169
- [26] Dobaczewski J, Magierski P, Nazarewicz, Satuła W, Szymański Z 2001 *Phys. Rev. C* **63**, 024308
- [27] Chowdhury D and Stauffer D 2000 *Principles of Equilibrium Statistical Mechanics* (Wiley-VCH, D-69469 Weinheim) p 285
- [28] Ehrenfest P 1933 *Leiden Commun. Suppl.* **75b**; 1933 *Proc. Akad. Wet.* **36**, 153
- [29] Blatt J M and Weisskopf V F 1952 *Theoretical Nuclear Physics* (Wiley, New York)
- [30] Bartholomew G A, Earle E D, Ferguson A J, Knowles J W, and Lone M A 1973 *Adv. Nucl. Phys.* **7**, 229
- [31] Gilbert A, Cameron A G W 1965 *Can. J. Phys.* **43**, 1446
- [32] Rauscher T, Thielemann F K, and Kratz K L 1997 *Phys. Rev. C* **56**, 1613

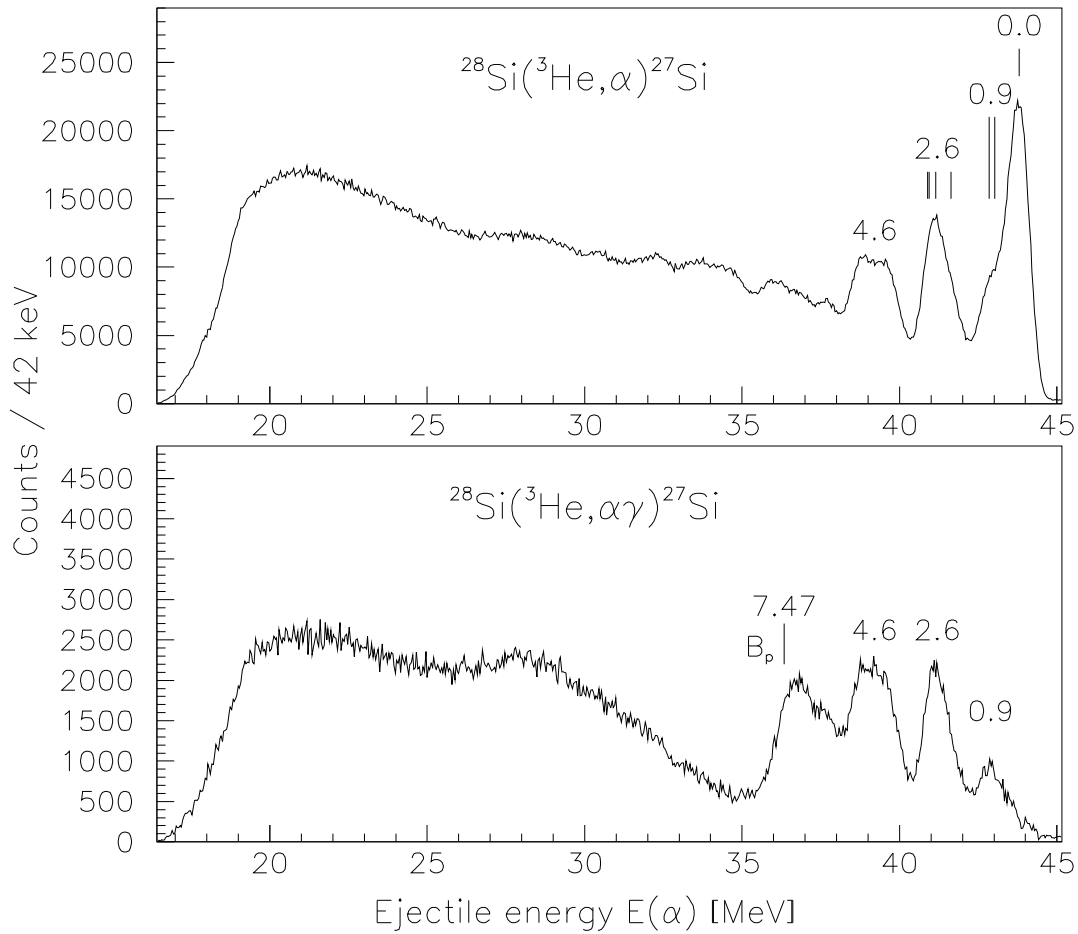


Figure 1. α -particles from the $^{28}\text{Si}(^3\text{He}, \alpha)$ reaction measured at 45° with respect to the beam axis and with a beam energy of 45 MeV. The lower panel shows the same spectrum, but in coincidence with one or more γ rays detected in the NaI detectors. Some known levels and the proton binding energy are indicated in MeV and by vertical lines.

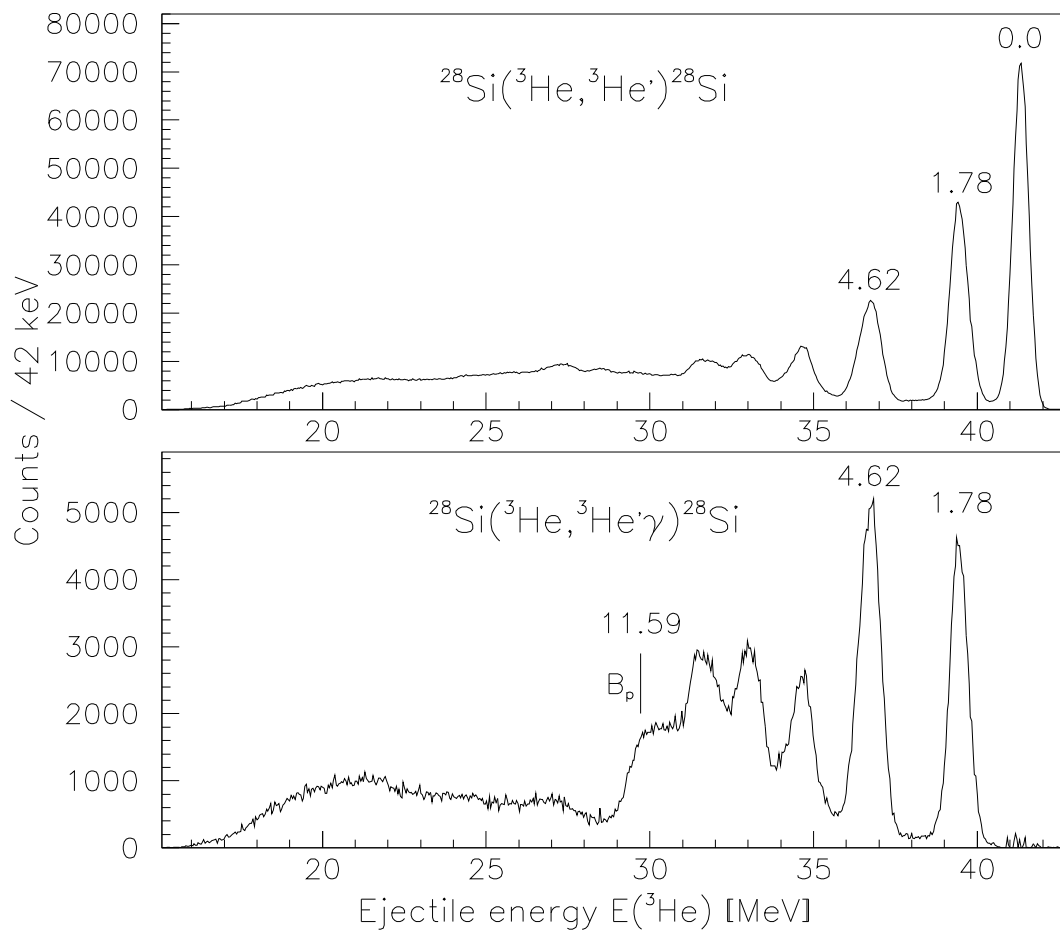


Figure 2. Same as figure 1, but ^3He particles from the $^{28}\text{Si}(^3\text{He}, ^3\text{He}')$ reaction.

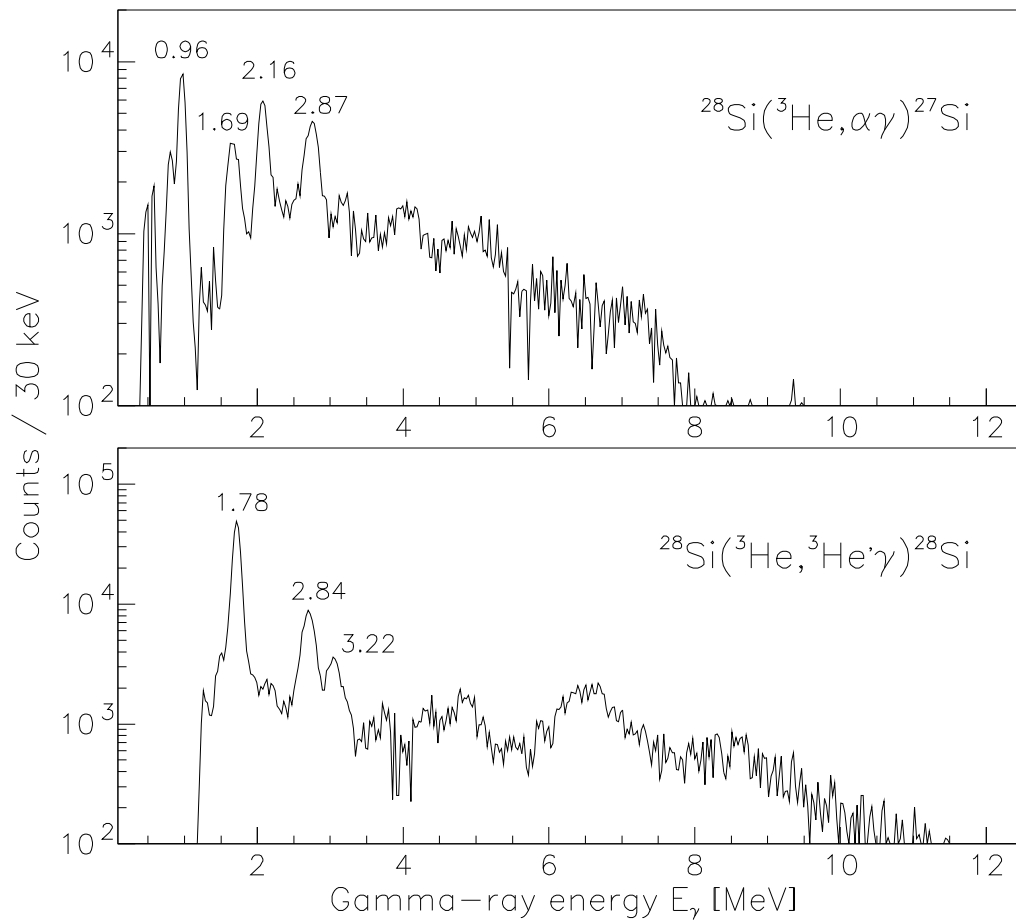


Figure 3. Unfolded NaI γ -ray spectra from ^{27}Si and ^{28}Si . The strongest γ lines are indicated by energies in MeV.

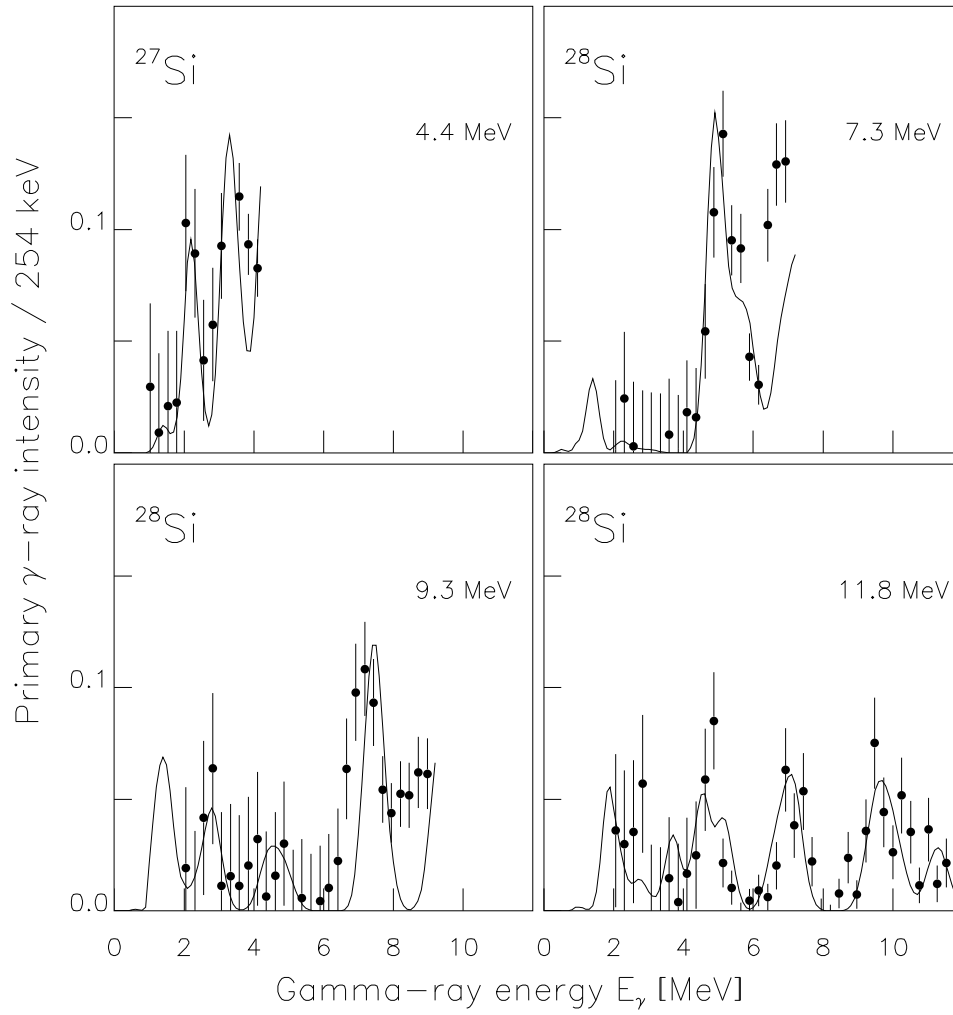


Figure 4. Comparison between primary γ -ray spectra extracted with our method (data points with error bars) and the spectra (solid lines) constructed from the known [14] γ -decay branching of levels around excitation energies indicated for each panel. The spectra are normalized to unity.

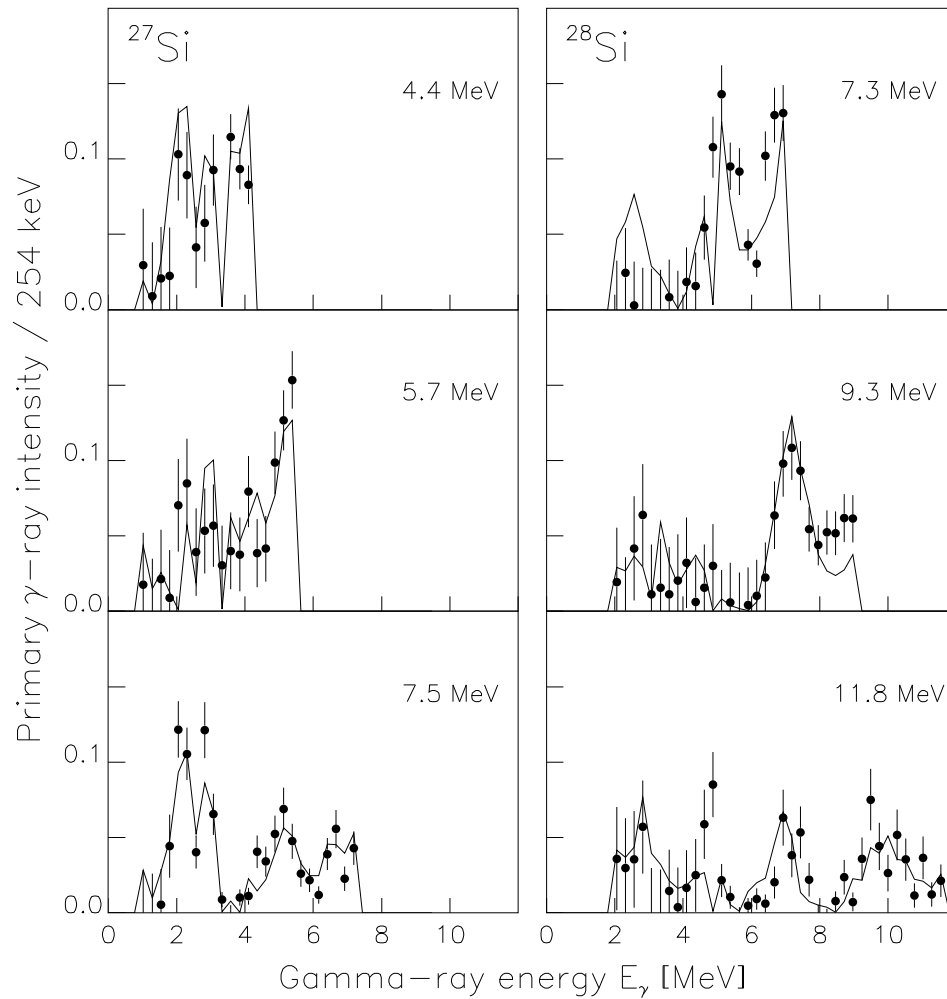


Figure 5. Comparison between experimental primary γ -ray spectra (data points with error bars) and the spectral distributions (solid lines) calculated from the extracted level density $\rho(E)$ and the γ -ray transmission coefficient $\mathcal{T}(E_\gamma)$. The initial excitation-energy bins are indicated in each panel. The spectra are normalized to unity.

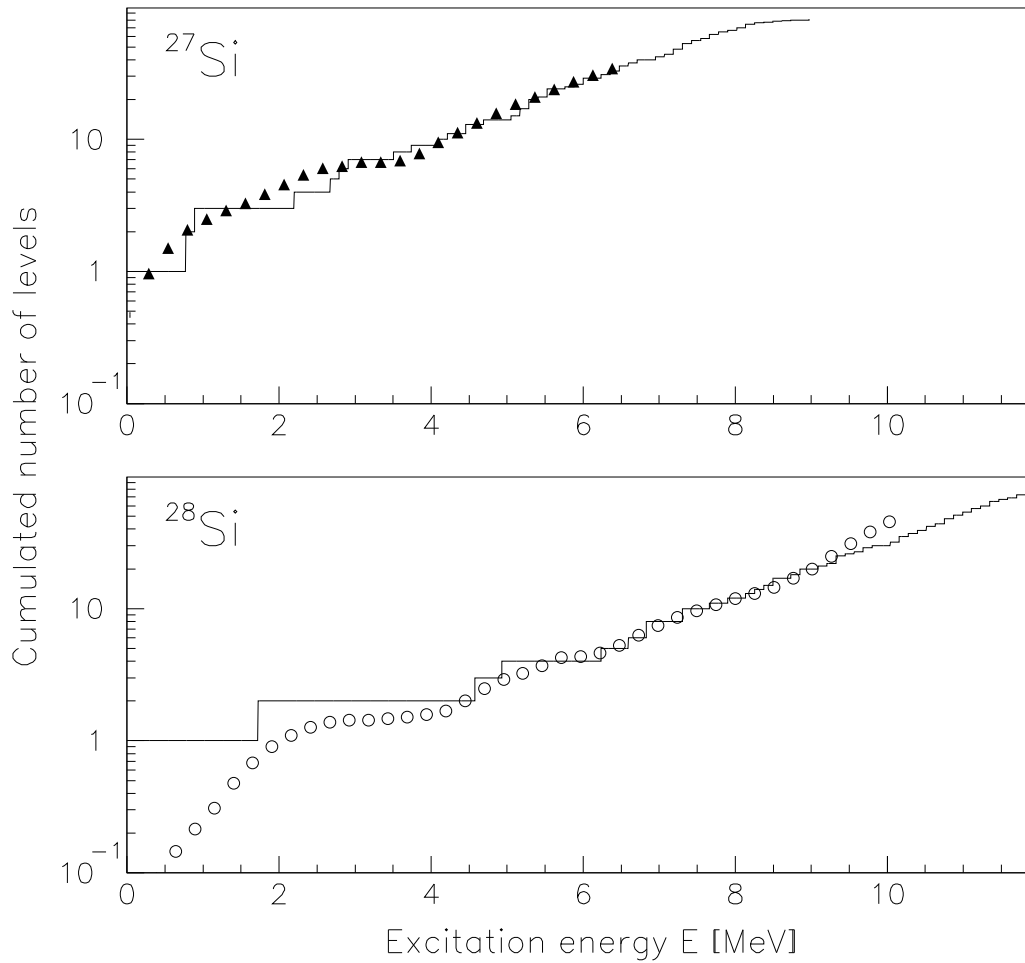


Figure 6. Cumulated number of levels with energy up to E in ^{27}Si and ^{28}Si . The extracted cumulative numbers (data points) are compared to values based on known levels (histogram). The extracted data for ^{28}Si at lower energies is underestimated due to the weak direct γ feeding of the ground state from $E = 4.2 - 12.1$ MeV of excitation energies.

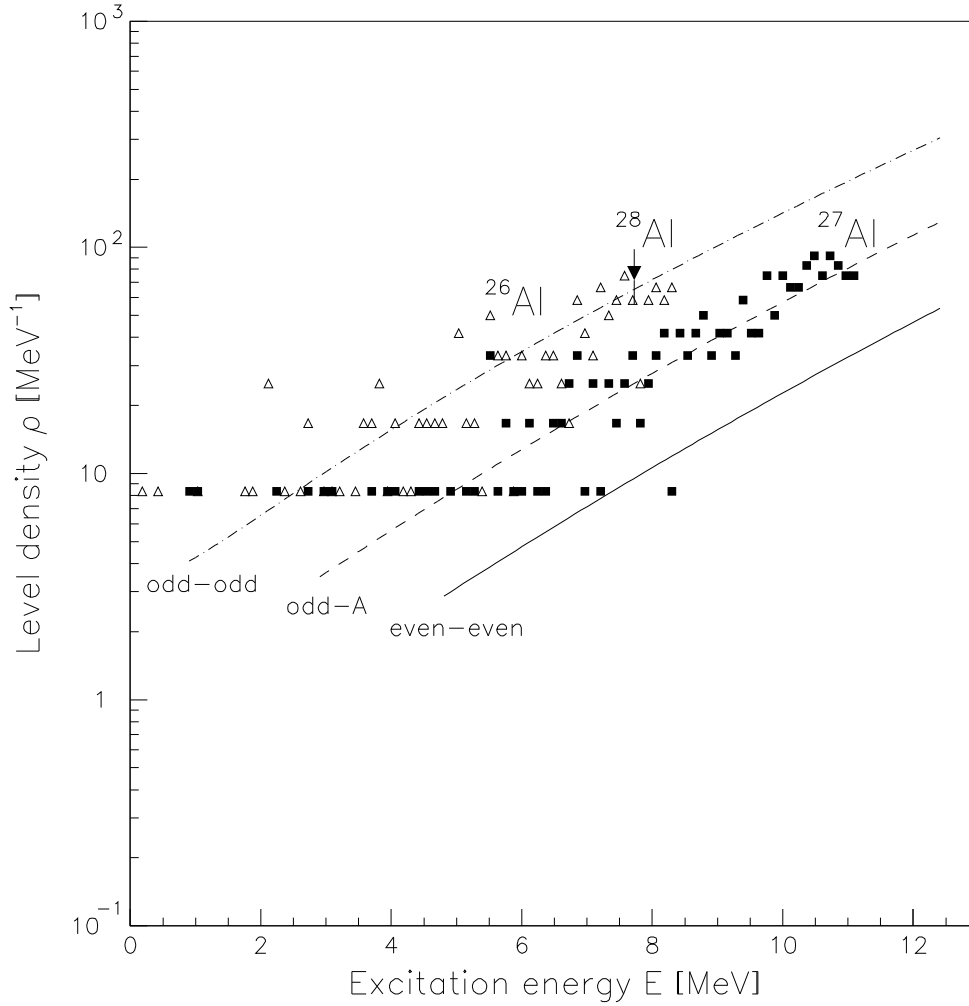


Figure 7. Level density in ^{26}Al (open triangles) and ^{27}Al (filled squares) determined by counting the number of known levels [14] within excitation energy bins of 120 keV. One data point (filled triangle with error bar) is based on neutron-resonance spacings in ^{28}Al [9, 24]. The model calculations (curves) are performed with the same parameter set for the even-even, odd- A and odd-odd systems: $\varepsilon = 2.0$ MeV, $\Delta = 2.3$ MeV, $r = 0.56$, $A_{\text{rot}} = 0.3$ MeV, $\hbar\omega_{\text{vib}} = 5.0$ MeV, and with seven proton and seven neutron pairs in the reservoir.

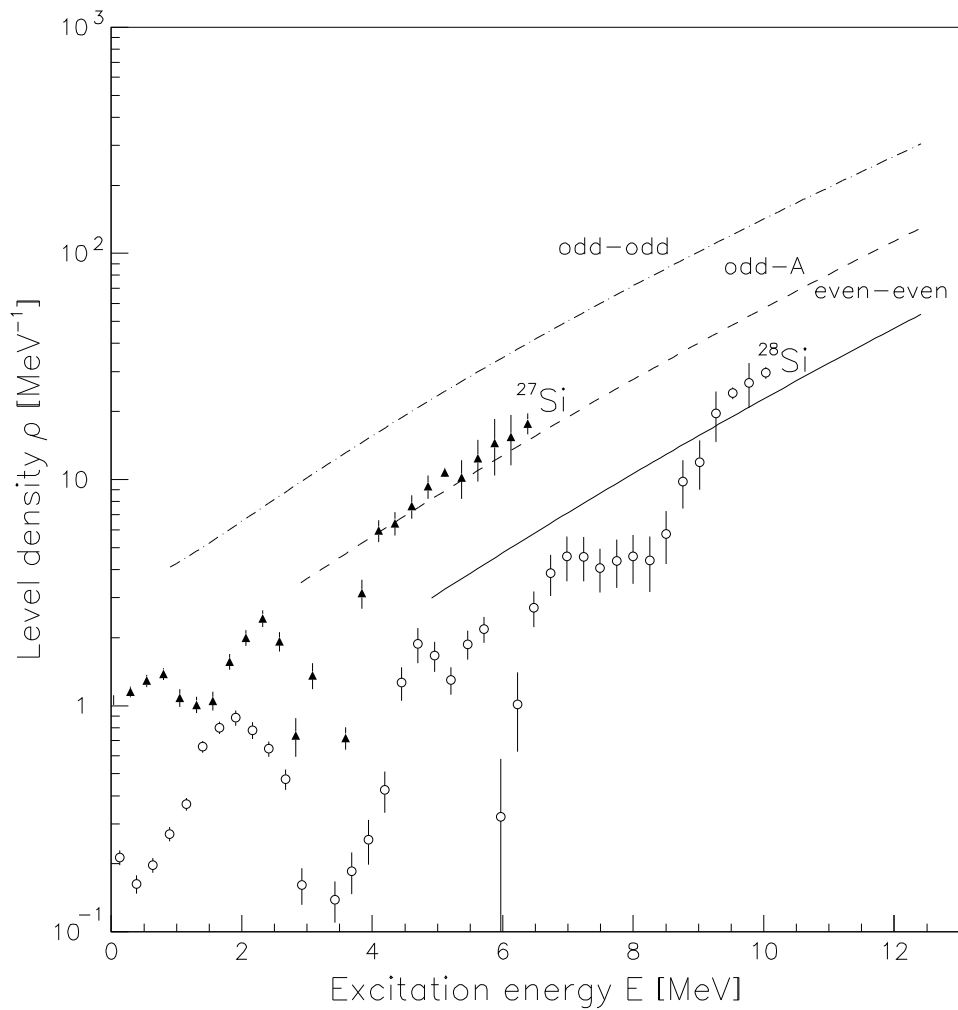


Figure 8. Comparison between level densities extracted from primary γ -ray spectra in ^{27}Si and ^{28}Si (data points) and model predictions (curves), see text of figure 7.

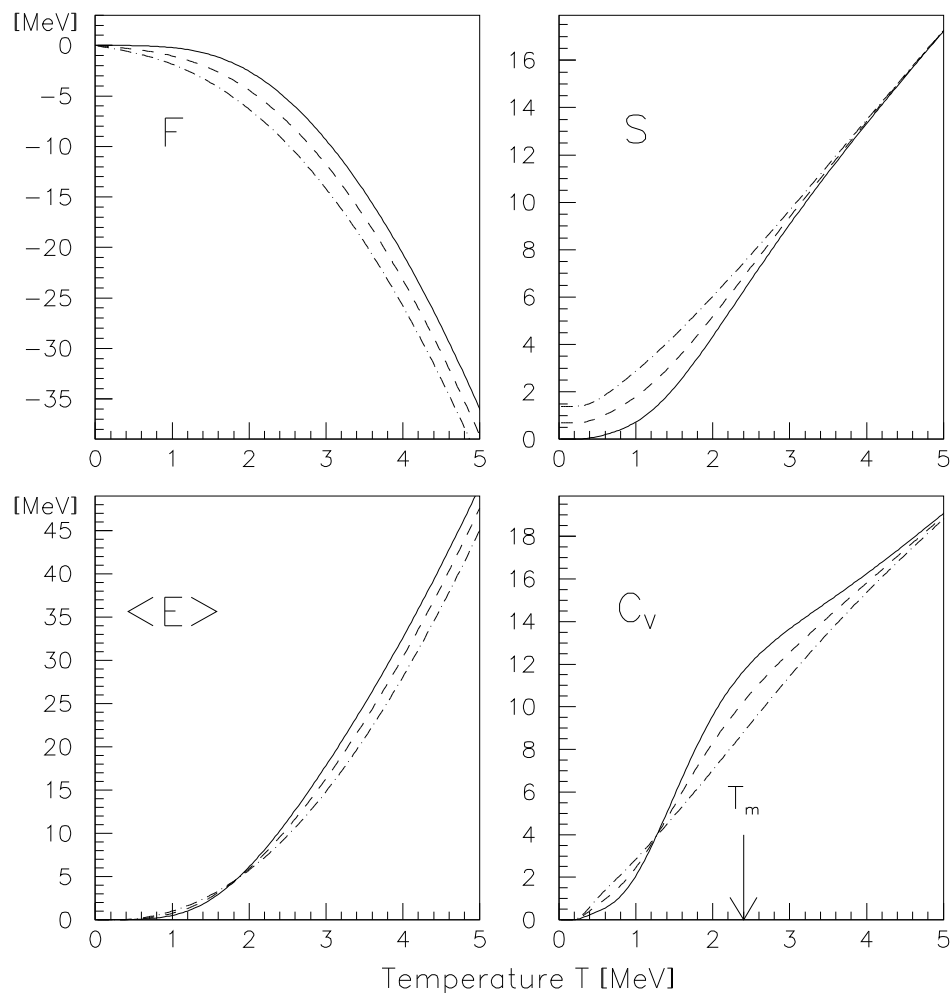


Figure 9. Model calculations for nuclei around ^{28}Si showing even-even (solid line), odd- A (dashed line) and odd-odd (dash-dotted line) systems. The four panels show the free energy F , the entropy S , the average excitation energy $\langle E \rangle$, and the heat capacity C_V as function of temperature T . The arrow at $T_m = 2.4$ MeV indicates the local maximum of C_V , where the pair breaking process is strong. The parameters are given in the text of figure 7.

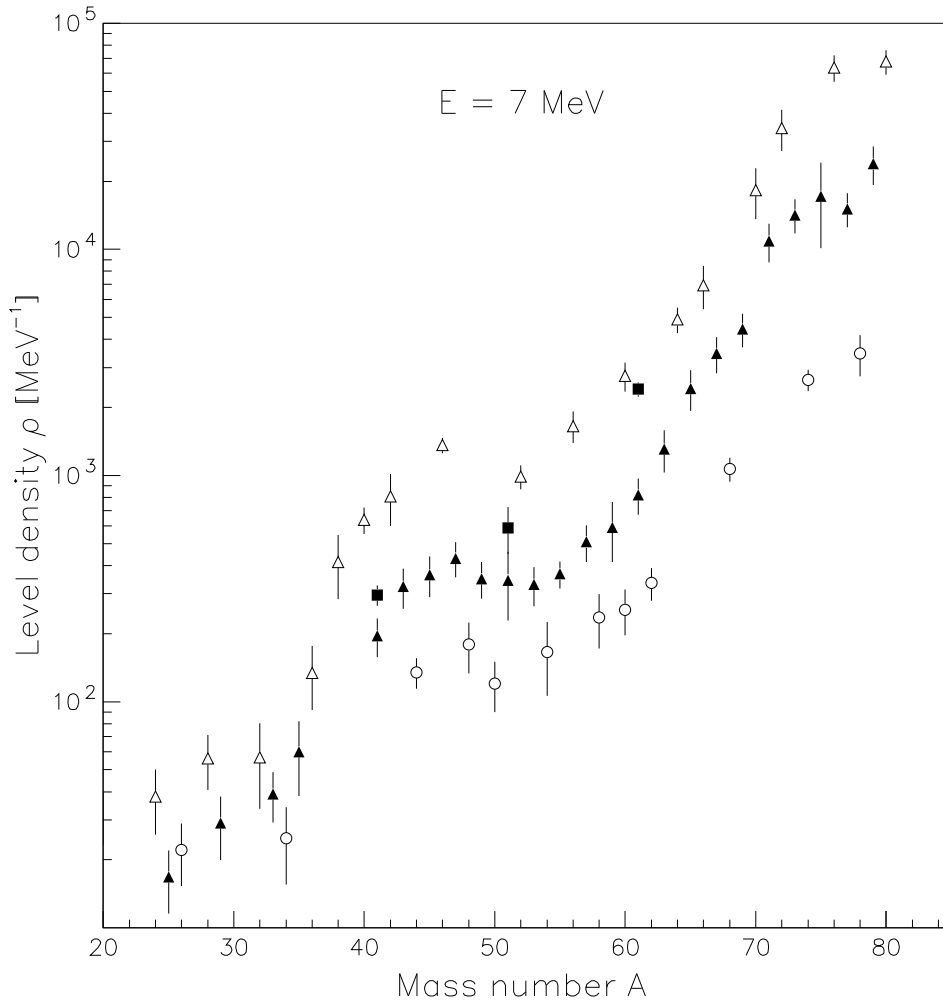


Figure 10. Level densities as function of mass number at 7 MeV excitation energy. The data are plotted for odd-odd (open triangles), odd-even (filled triangles), even-odd (filled squares), and even-even (open circles) nuclei. The data are extracted from experimental values, as described in [9].

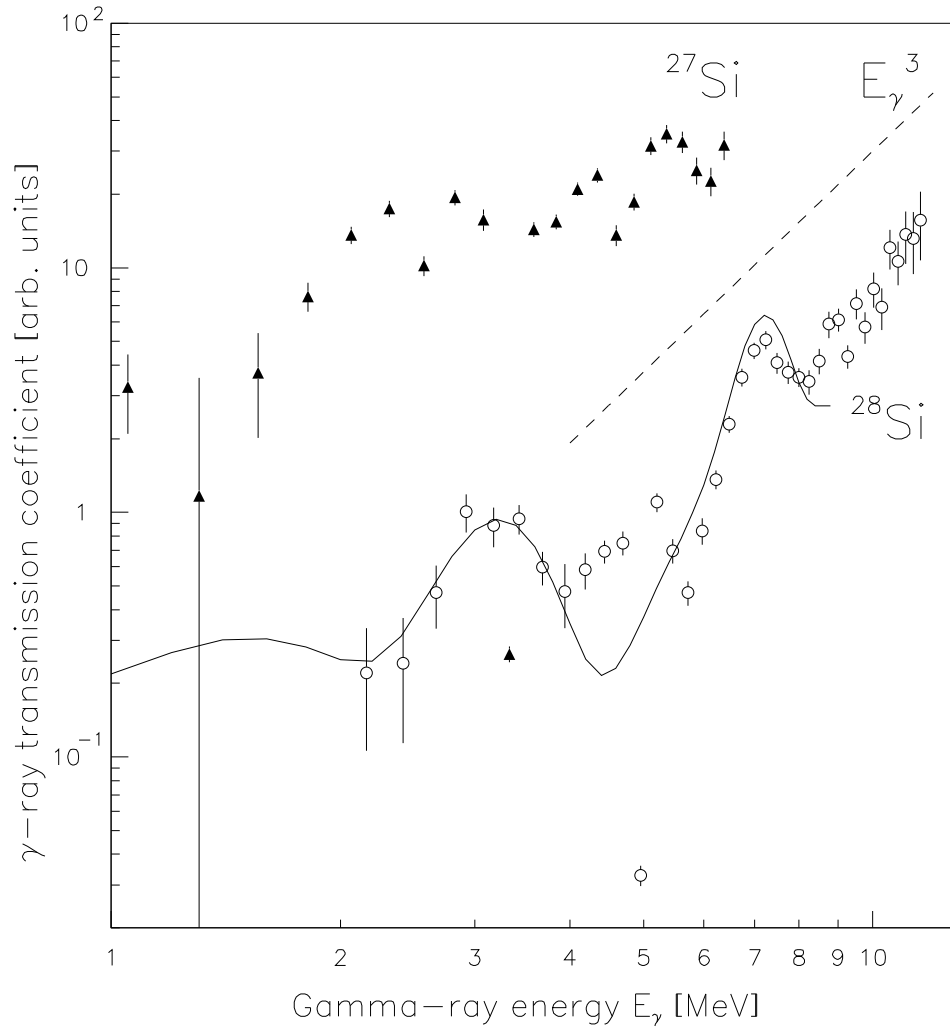


Figure 11. Extracted γ -ray transmission coefficient $\mathcal{T}(E_\gamma)$ in ^{27}Si and ^{28}Si (not normalized). The solid line is determined (see text) from γ transitions depopulating levels in ^{28}Si with known lifetimes [14]. The slopes of the transmission coefficients follow very roughly a $\sim E_\gamma^3$ dependency (dashed line).